Mechanism of Activation and Selectivity in a Ligand-Gated Ion Channel: Structural and Functional Studies of GluR2 and Quisqualate[†,‡]

Rongsheng Jin,[§] Michelle Horning,[∥] Mark L. Mayer,[∥] and Eric Gouaux*[,§,⊥]

Howard Hughes Medical Institute and Department of Biochemistry and Molecular Biophysics, Columbia University, New York, New York 10032, and Laboratory of Cellular and Molecular Neurophysiology, National Institute of Child Health and Human Development, National Institutes of Health, Bethesda, Maryland 20892

Received September 10, 2002; Revised Manuscript Received October 29, 2002

ABSTRACT: Glutamate is the major excitatory neurotransmitter in the mammalian brain. The (*S*)-2-amino-3-(3-hydroxy-5-methyl-4-isoxazole)propionic acid (AMPA)-subtype glutamate receptor, a ligand-gated ion channel, mediates most of the fast excitatory synaptic transmission in the mammalian central nervous system. Here we present electrophysiological, biochemical, and crystallographic data on the interactions between quisqualate and the GluR2 receptor ion channel and its corresponding ligand binding core. Quisqualate is a high-affinity, full agonist which like AMPA and glutamate elicits maximum peak current responses, and stabilizes the ligand binding core in a fully closed conformation, reinforcing the concept that full agonists produce similar conformational changes [Armstrong, N., and Gouaux, E. (2000) *Neuron 28*, 165−181]. Nevertheless, the mechanism of quisqualate binding is different from that of AMPA but similar to that of glutamate, illustrating that quisqualate is a faithful glutamate analogue. A detailed comparison of the three agonist complexes reveals distinct binding mechanisms, particularly in the region of a hydrophobic pocket that is proximal to the anionic γ-substituents, and demonstrates the importance of agonist−water−receptor interactions. The hydrophobic pocket, which is predicted to vary in chemical character between receptor subtypes, probably plays an important role in determining receptor subtype specificity.

Excitatory synapses in the central nervous system (CNS) release glutamate onto postsynaptic sites populated by ionotropic glutamate receptors (iGluRs).[1] The three primary subgroups of iGluRs are the AMPA, *N*-methyl-D-aspartate (NMDA), and kainate receptors, although a prokaryotic, "minimal" homologue has recently been discovered and characterized (*1*, *2*). The eukaryotic receptors were originally defined by their agonist selectivity, a definition that was subsequently reinforced by the amino acid sequence of their respective polypeptides (*3*−*5*). Recent evidence suggests that iGluRs are homo- or heterotetramers composed of subfamily specific subunits, assembled as a pair of dimers (*2*, *6*−*10*). Eukaryotic iGluR subunits are each composed of an amino-terminal domain (ATD), a ligand-binding core (S1S2), three transmembrane segments (1−3), a reentrant pore loop (P), and an intracellular carboxy-terminal tail (*11*−*15*), as illustrated in Figure 1.

By taking advantage of the modular construction of iGluRs, we have defined a S1S2 construct of the GluR2 ligand-binding core, the so-called S1S2J variant (*7*), that recapitulates the binding properties of the full-length receptor and is amenable to high-resolution structural analysis, to biochemical and biophysical studies, and to analysis by NMR spectroscopy (*16*−*19*). Recently, we have carried out a series of structural and functional studies on the GluR2 receptor and the S1S2J ligand-binding core aimed at elucidating mechanisms for agonist and antagonist binding, and receptor activation and desensitization (*7*, *20*). On the basis of these experiments, we suggest that unique chemical and structural features of GluR2 agonists are detected by key residues in and around the ligand-binding pocket and that, depending on the specific interactions, the binding of different ligands may lead to different protein conformations, which in turn may be coupled to differential activation and desensitization of the ion channel. To determine the extent to which the aforementioned hypothesis is valid, we have carried out functional and structural analyses of the GluR2 receptor and its ligand-binding core with full and partial agonists. Here we present results from studies with quisqualate.

[†] This work was supported by the National Institutes of Health (E.G. and M.L.M.) and the National Alliance for Research on Schizophrenia and Depression. E.G. is a Klingenstein Fellow and an assistant investigator with the Howard Hughes Medical Institute.

[‡] Coordinates for the non-zinc and zinc form quisqualate complexes with GluR2 S1S2 have been deposited with the Protein Data Bank as entries 1MM6 and 1MM7, respectively.

* To whom correspondence should be addressed. E-mail: jeg52@columbia.edu. Phone: (212) 305-4475. Fax: (212) 305-8174.

[§] Department of Biochemistry and Molecular Biophysics, Columbia University.

[∥] National Institutes of Health.

[⊥] Howard Hughes Medical Institute, Columbia University.

[1] Abbreviations: iGluRs, ionotropic glutamate receptors; GluR2, ionotropic glutamate receptor subtype 2 or B; AMPA, (*S*)-2-amino-3-(3-hydroxy-5-methyl-4-isoxazole)propionic acid; NMDA, *N*-methyl-D-aspartate; ATD, amino-terminal domain; S1S2, GluR2 ligand-binding core; NMR, nuclear magnetic resonance; GluR2 S1S2J, ligand-binding core construct employed in this study; GluR2 L483Y, leucine to tyrosine mutant of GluR2 at position 483; PEG, polyethylene glycol; ncs, noncrystallographic symmetry; rmsd, root-mean-square deviation; NSLS, National Synchrotron Light Source; quisqualate, (*S*)-2-amino-3-(3,5-dioxo-1,2,4-oxazadiazolindin-2-yl)propionic acid; HEK, human embryonic kidney.

10.1021/bi020583k CCC: $22.00
Published on Web 12/04/2002

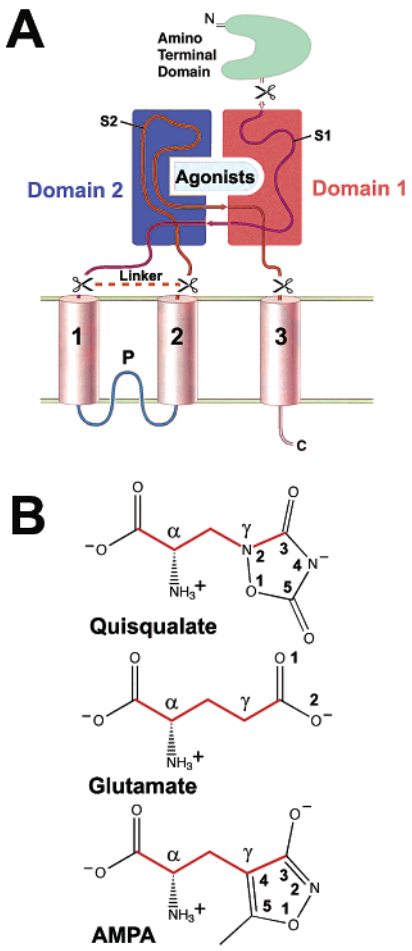

FIGURE 1: iGluR domain organization and agonist structure. (A) The S1 and S2 polypeptide segments, linked together by a dipeptide linker, comprise the water-soluble ligand-binding core employed in the studies described here. The scissors and "Linker" indicate where S1 and S2 begin and end and where S1 is connected to S2, respectively. (B) Chemical structures of quisqualate, glutamate, and AMPA.

(*S*)-Quisqualic acid, isolated from the seeds of *Quisqualis indica* and *Quisqualis fructus*, is an anthelmintic and the active compound in the Chinese herbal drug Shihchuntz (*21*). Quisqualic acid is an α-amino acid that incorporates a 1,2,4-oxadiazolidine ring into the γ-position rather than the simple carboxylate of glutamate, as indicated in Figure 1. Also like glutamate, quisqualate was shown nearly 30 years ago to activate putative glutamate receptors (*22*). Subsequent experiments showed that the non-NMDA receptors activated by quisqualate could be divided into two different groups: so-called quisqualate and kainate receptors (*23*). However, like glutamate, quisqualate elicits at least partial activation at all three subfamilies of the eukaryotic iGluRs (*24*), and in addition activates G-protein-coupled glutamate receptors (*25*). Thus, AMPA, which has greater subfamily specificity, became the namesake of the GluR1−GluR4 (alternatively GluRA−GluRD, respectively) or AMPA receptors (*26*).

The structures of the GluR2 S1S2J ligand-binding core in complex with the full agonists glutamate and AMPA show that domain 1 and domain 2 close by ∼20° in the transition from the apo to the full agonist-bound state, while partial agonists induce less domain closure (*7*). Even though glutamate and AMPA give a similar degree of domain closure, and they result in similar levels of channel activation, the γ-substituents of glutamate and AMPA bind to the receptor cleft in strikingly different modes (*7*). To gain a better understanding of the molecular basis for agonist selectivity, receptor subtype specificity, and the relationships between the mode of agonist binding, domain closure, and receptor activation, we have undertaken a series of physiological, biochemical, and crystallographic studies with the GluR2 receptor and its ligand-binding core. The results from the experiments with quisqualate presented herein, in combination with additional data gleaned from previous functional and structural studies, will assist in the design of novel glutamate receptor ligands and may lead to compounds with subfamily selective properties.

EXPERIMENTAL PROCEDURES

Materials. L-Glutamate and (*S*)-quisqualate were employed in this study and were obtained from Sigma and Research Biochemicals, respectively. The plasmid, pS1S2J, used to express the GluR2 S1S2J protein was from the Gouaux laboratory; [^{3}H]AMPA was from New England Nuclear, and all other reagents were reagent grade or higher.

Protein Purification. The rat GluR2 S1S2J construct used in this study was derived from GluR2 (flop) (*4*, *27*) and includes Asn392−Lys506 (S1) and Pro632−Ser775 (S2), with the two segments connected by a Gly-Thr dipeptide linker (*7*). Protein expression, refolding, and purification were performed as previously described (*16*, *17*, *28*). Before crystallization, the protein was dialyzed extensively to remove residual glutamate using a buffer composed of 10 mM HEPES (pH 7.0), 20 mM NaCl, and 1 mM EDTA.

Ligand Binding Assay. The activity assay was carried out in the following buffer: 30 mM Tris-hydrochloride (pH 7.2), 100 mM potassium thiocyanate, 2.5 mM calcium chloride, and 10% glycerol (*13*). For competition binding studies, 20 nM [^{3}H]AMPA (10.6 Ci/mmol) was incubated with various concentrations of quisqualate (from 1 nM to 100 μM). GSWP 02500 membranes were used for filter binding. The extent of nonspecific binding was determined in the presence of 1 mM glutamate. Ligand binding experiments were carried out in duplicate, and the reported results are the average of the two experiments.

Crystallization and Data Collection. The protein was concentrated to ∼10 mg/mL for crystallization and then supplemented with 5 mM quisqualate. Crystals were grown at 4 °C by vapor diffusion, and each drop contained a 1:1 ratio of protein and reservoir solution. The reservoir solution for the zinc form crystals was 10−15% PEG 8000, 0.1 M zinc acetate, and 0.1 M sodium acetate (pH 5.5); the non-zinc form was obtained from a reservoir solution composed of 16−20% PEG 8000, 0.15−0.2 M ammonium sulfate, and 0.1 M sodium citrate (pH 5.5).

All diffraction data were collected at 110 K, and the cryo buffers were supplemented with ligand and 12−16% glycerol. The data set for the zinc form was collected at NSLS X4A, and the non-zinc diffraction data set was obtained using Cu Kα radiation and an R-Axis IV detector. The diffraction data were processed with the HKL suite of programs (*29*). The zinc form crystals belong to the $P2_12_12$ space group, and the cell is isomorphous to the AMPA/glutamate crystal form (*7*). The non-zinc form quisqualate crystals also belong to the $P2_12_12$ space group, but with different unit cell dimensions and molecular packing.

Structure Determination and Analysis. The structure of the zinc form quisqualate complex was determined by difference Fourier techniques using phases calculated from the zinc form AMPA structure (*7*). The non-zinc form quisqualate structure was determined by molecular replacement with AMoRe (*30*) using the fluorowilliardiine complex structure without solvent molecules and ligand as a search model (R. Jin and E. Gouaux, unpublished results). Crystallographic refinements were performed with CNS (*31*), and the program O was used for model building (*32*, *33*). Refinements were begun with rigid body minimization followed by a slow-cool simulated annealing protocol at 5000 K to reduce model bias. Iterative rounds of positional and individual *B*-factor refinement were performed in conjunction with model building into omit maps until R_{free} (*34*) converged. The ligands were not included until R_{free} was <0.30. Least-squares superpositions were calculated using LSQMAN (*35*), and the extent of domain closure was determined using the program FIT (*36*). The extent of domain closure was defined as the rotation required to fit domain 2 following superposition of domain 1 when the Cα atoms were used. MOLSCRIPT (*37*), BOBSCRIPT (*38*), and Raster3D (*39*) were used to make the figures.

Physiology. RNA encoding the unedited rat GluR2 (flip) (also known as GluRB) (*40*) L483Y receptor (0.5 ng) was injected into the cytoplasm of oocytes from *Xenopus laevis*. Experiments were performed under two-electrode voltage clamp (Axoclamp 2A) at a holding potential of −60 mV using agarose-cushioned electrodes filled with 3 M KCl (*41*). The oocyte was continuously perfused in a modified Barth's solution [100 mM NaCl, 1 mM KCl, 0.5 mM $BaCl_2$, 1 mM $MgCl_2$, and 5 mM HEPES (pH 7.6)], to which agonists were added as required. The EC_{50} values, determined for the same GluR2 L483Y construct, were 1.2 μM for quisqualate and 20 μM for glutamate; the agonist concentrations used to evoke maximum responses were 100 μM quisqualate and 2 mM glutamate. Recordings were repeated on nine different oocytes. For rapid perfusion experiments, HEK 293 cells grown on 35 mm dishes were transfected with 3 μg of cDNA. Recordings were performed at room temperature using an Axopatch 200A amplifier and outside-out patches positioned in front of four-bore glass tubing mounted on a P245.30 piezoelectric stack driven by a P-270 HVA amplifier (Physik Instrumente). The external solution contained 145 mM NaCl, 2.5 mM KCl, 1.8 mM $CaCl_2$, 1 mM $MgCl_2$, 5 mM HEPES (pH 7.3), and 10 mM glucose. The internal solution contained 110 mM NaF, 10 mM NaCl, 5 mM Na_4BAPTA, 0.5 mM $CaCl_2$, 10 mM MgATP, and 5 mM HEPES (pH 7.2). To maximize the rate of receptor activation by agonists, glutamate and quisqualate were applied at concentrations of 10 and 3 mM, respectively. Recordings were repeated on 12 different patches, 11 for quisqualate, and 8 for glutamate. Current responses were acquired by an ITC-16 interface (Instrutech Corp.) under control of the program Synapse (Synergistic Research Systems). Data were analyzed and graphed using KaleidaGraph.

RESULTS

Quisqualate Is a High-Affinity Full Agonist. In a ligand binding competition assay with [^{3}H]AMPA and the GluR2 S1S2J construct, quisqualate yielded an IC_{50} of 20 nM, as illustrated in Figure 2. In comparison, the previously reported

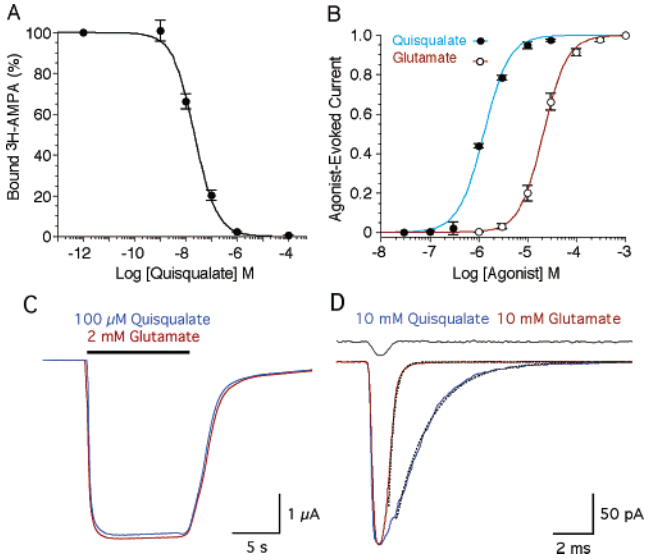

FIGURE 2: Quisqualate is a high-affinity, full agonist on the GluR2 receptor. (A) Competition by quisqualate for [^{3}H]AMPA binding as assayed by a filter binding assay. The IC_{50} value is 20.0 nM. (B) Concentration response curves for activation of the nondesensitizing L483Y mutant of the GluR2 receptor by quisqualate and glutamate; data points shown are means ± the standard error of the mean of responses from two electrode voltage clamp experiments performed on five oocytes. (C) Records from a representative experiment with saturating concentrations of 2 mM glutamate and 100 μM quisqualate applied to a single oocyte for 10 s. (D) Responses of the same membrane patch from a HEK cell expressing wild-type GluR2 to 1 ms applications of 10 mM quisqualate or glutamate; the top trace shows the open tip junction current recorded at the end of the experiment, and dotted lines show the fit of single-exponential functions of time constants of 1.75 and 0.27 ms for quisqualate and glutamate, respectively.

quisqualate IC_{50} values for longer GluR2 S1S2 and GluR4 S1S2 constructs expressed in *Escherichia coli* were 11 and 22 nM, respectively (*42*). For the full-length GluR2 receptor expressed in insect cells, the corresponding IC_{50} value for quisqualate competition with [^{3}H]AMPA binding was 9 nM (*43*). In contrast, L-glutamate [IC_{50} = 166 nM (*16*)] binds to the GluR2 S1S2J construct with an 8.3-fold lower affinity than quisqualate. Like glutamate, quisqualate also potently activates the GluR2 ion channel. Dose−response analysis by two-electrode voltage clamp on *Xenopus* oocytes expressing the L483Y nondesensitizing GluR2 point mutant (*44*) yielded an EC_{50} of 1.2 μM, while for glutamate, the EC_{50} equaled 20 μM (Figure 2). To compare the extent to which glutamate and quisqualate activate the GluR2 ion channel, we then recorded the responses to saturating concentrations of quisqualate and glutamate (ca. 100-fold above their EC_{50} values) from the same cells, also using the L483Y variant of GluR2. As shown in Figure 2, quisqualate has an efficacy similar to that of glutamate and produces comparable amplitude peak responses. However, as a consequence of the higher affinity of quisqualate, the agonist−receptor complex is more stable than that for glutamate. As a result, when applied for 1 ms the rate at which channels close following the removal of agonist is 6-fold slower for quisqualate [$k_{off} = 474 \pm 44\ s^{-1}$ ($n = 11$)] than for glutamate [$k_{off} = 2758 \pm 257\ s^{-1}$ ($n = 8$)] for responses measured from wild-type GluR2. In the continued presence of agonists, GluR2 responses to quisqualate and glutamate show strong desensitization, which proceeds at a

Table 1: Data Collection Statistics

ligand	space group	unit cell dimensions (Å)	no. per AU[a]	λ (Å)	d_{min} (Å)[b]	mean redundancy	R_{merge} (%)[c,d]	completeness (%)[d]
Quis	$P2_12_12$	$a = 98.56$, $b = 121.53$, $c = 47.45$	2	1.54	2.15 (2.25)	3.39	5.5 (12.9)	90.3 (59.9)
Quis-Zn	$P2_12_12$	$a = 113.91$, $b = 163.45$, $c = 47.34$	3	0.9879	1.65 (1.71)	5.64	5.1 (19.7)	90.1 (53.5)

[a] Number of protein molecules per asymmetric unit (AU). [b] Values in parentheses define the low-resolution limits for the last shell of data. [c] $R_{merge} = (\Sigma|I_i - \langle I_i\rangle|)/\Sigma|I_i|$, where $\langle I_i\rangle$ is the mean I_i over all symmetry-equivalent reflections. [d] Values in parentheses are statistics for the last shell of data.

Table 2: Refinement Statistics

ligand	resolution (Å)	R_{work}[a] (%)	R_{free}[b] (%)	no. of protein atoms	no. of waters	no. of ligand atoms	average *B* value: overall	average *B* value: main chain	average *B* value: ligand	rms deviation: bonds (Å)	rms deviation: angles (deg)	rms deviation: *B* value: bonds	rms deviation: *B* value: angles
Quis	30−2.15	19.0	23.7	3995	442	26	21.34	19.42	13.59	0.005	1.163	1.268	1.961
Quis-Zn	30−1.65	20.4	23.7	5855	774	39	18.06	15.67	12.03	0.011	1.445	1.834	2.718

[a] $R_{work} = (\Sigma|F_o| - |F_c|)/\Sigma|F_o|$, where F_o and F_c are the observed and calculated structure factors, respectively. [b] The reflections which were set aside for the calculation of the R_{free} value were 10 and 5% for the non-zinc crystal form and zinc crystal form, respectively.

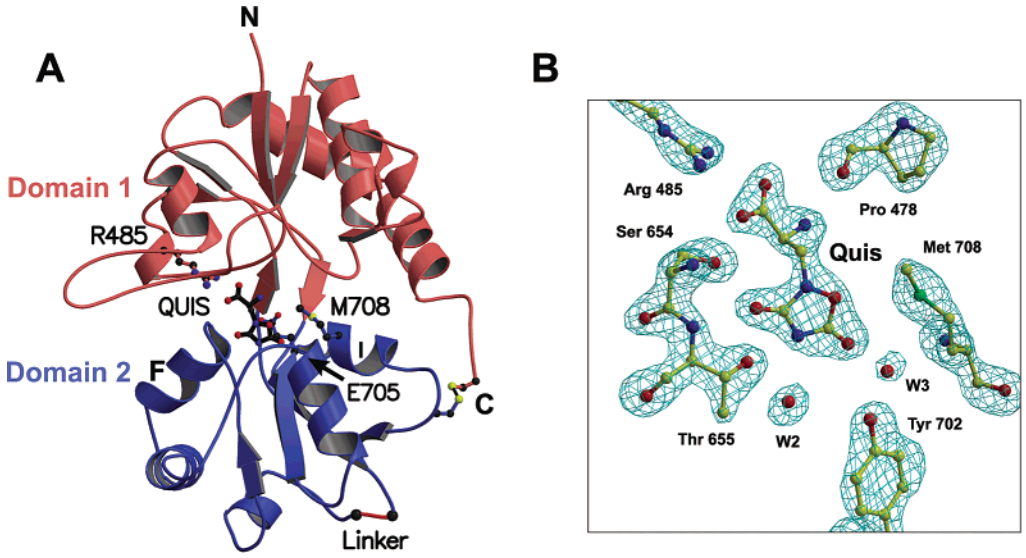

FIGURE 3: Quisqualate binds in the cleft between domains 1 and 2 and has well-defined electron density. (A) Ribbon representation of the GluR2 ligand-binding core in complex with quisqualate. Domain 1 is pink, and domain 2 is blue. Quisqualate, key binding site residues R485, M708, and E705, helices F and I, and the dipeptide linker are labeled. Note that the linker connecting S1 and S2 is within domain 2 and is not between domain 1 and domain 2. (B) An "omit" $F_o - F_c$ electron density map of quisqualate together with the selected surrounding residues and water molecules W2 and W3. The map is contoured at 4.0σ.

similar rate for both agonists [$k_{des} = 216 \pm 16$ s^{-1} ($n = 12$) for quisqualate, and $k_{des} = 190 \pm 15$ s^{-1} ($n = 8$) for glutamate], indicating that there is a rate-limiting conformational step, which may be rearrangment of the ligand-binding core dimer interface (*20*). The k_{off}/k_{des} ratio is 15 ± 1.3 for glutamate but only 2.2 ± 0.08 for quisqualate, indicating that during a single turnover receptors which have bound quisqualate have a high probability of entering the desensitized state, while for glutamate, receptors preferentially return to the ground state without desensitizing.

Quisqualate Induces the Same Domain Closure as Glutamate and AMPA. We have determined the structure of the GluR2 S1S2J ligand-binding core in complex with quisqualate in two different crystal forms: a so-called zinc form and a non-zinc form. Documented in Tables 1 and 2 are the relevant crystallographic statistics. The zinc form crystals are isomorphous to the AMPA/glutamate crystals (*7*), while the non-zinc form crystals represent a new lattice. There are three molecules in an asymmetric unit of the zinc form, two of which form a noncrystallographic symmetry (ncs)-related dimer, while the third molecule forms a dimer with the crystallographic symmetry equivalent molecule in an adjacent asymmetric unit. Forming important lattice interactions in the zinc form crystals are five zinc ions; four ions mediate interprotomer interactions, while the fifth is bound to protomer C via intramolecular interactions (*7*). The non-zinc crystal form has an ncs dimer in the asymmetric unit, and there are relatively few protein−protein, interdimer interactions in this lattice. Therefore, the possible perturbations of receptor conformation due to lattice interactions are fewer in number in the non-zinc form than in the zinc crystal form.

Quisqualate binds between domain 1 and domain 2 and induces an extent of domain closure similar to those of glutamate and AMPA. Shown in Figure 3 is the complex of GluR2 S1S2J and quisqualate. Indeed, the five crystallographically independent complexes have essentially identical structures. Superposition of the two ncs-related protomers in the non-zinc form yields a root-mean-square deviation (rmsd) of 0.35 Å for α-carbon atoms. Additional superposi-

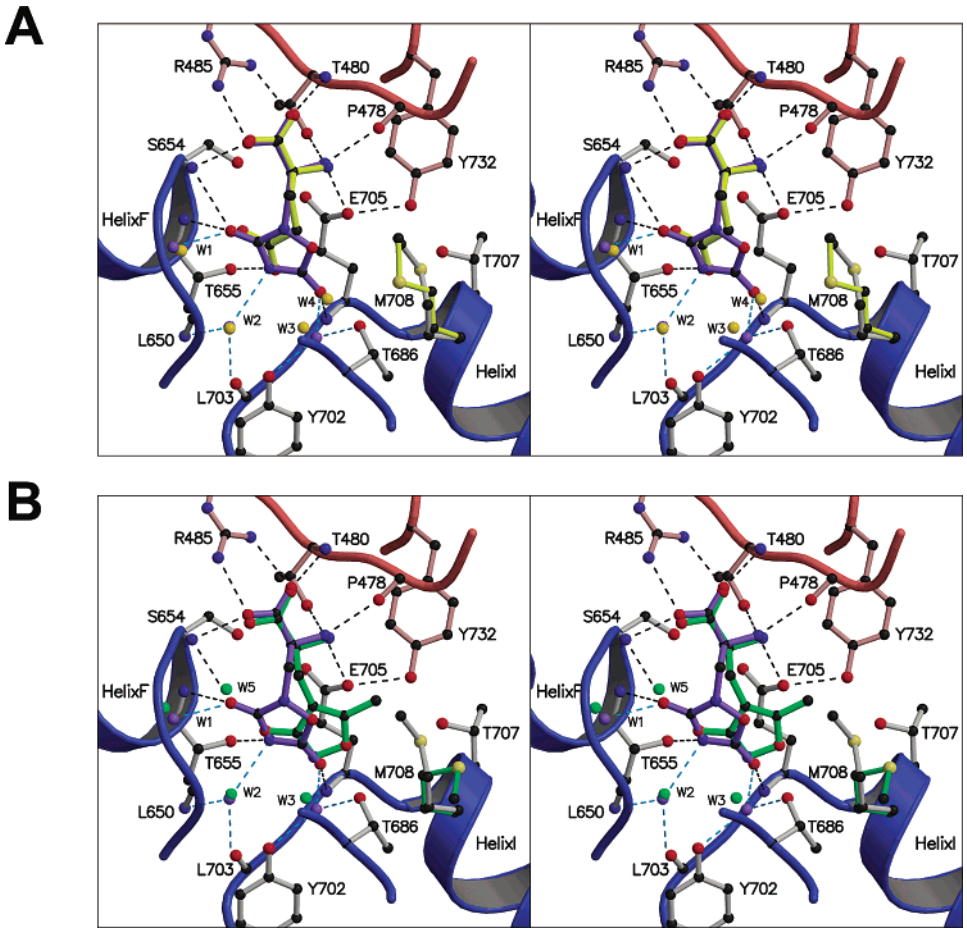

FIGURE 4: Comparisons of the interactions between the GluR2 S1S2J ligand-binding core and quisqualate, glutamate, and AMPA. (A) Stereoview of the binding pocket in superimposed quisqualate and glutamate structures, in which the α-carbon atoms of domain 1 were employed for the superposition. Main chain segments for the quisqualate structure are in pink (domain 1) and blue (domain 2), and side chain and quisqualate atoms are shown in ball-and-stick representation (black for carbon, blue for nitrogen, red for oxygen, and yellow for sulfur). Bonds for the protein residues are pink for domain 1 and gray for domain 2. Quisqualate is in purple. Glutamate is drawn in yellow, and the side chain of M708, from the glutamate complex, is also in yellow. With the exception of M708, no other protein atoms from the glutamate complex are shown. Water molecules are shown as spheres and are colored purple for the quisqualate complex and yellow for the glutamate complex. Hydrogen bonds are shown as dashed lines; direct interactions to the protein are in black, and water-mediated interactions are in blue. (B) Stereoview of the binding pocket in superimposed quisqualate and AMPA structures. The quisqualate structure and hydrogen bonds are colored as in panel A. The ligand, four conserved water molecules, and residue M708 in the AMPA complex are green.

tions show that the average rmsd between the zinc form and non-zinc form structures is 0.40 Å for α-carbon atoms. Superpositions of the quisqualate-bound GluR2 S1S2J with the corresponding glutamate or AMPA complexes gave rms deviations of 0.34 and 0.32 Å, respectively, and calculations using the program FIT did not provide any evidence for significant differences in domain closure between the quisqualate, glutamate, and AMPA complexes. Taken together, these results show that the three full agonist protein structures are very similar and that quisqualate binding induces the same extent of domain closure as glutamate and AMPA.

Quisqualate Adopts a Distinct Binding Mode. As illustrated in Figure 3, the electron density associated with quisqualate is well-defined and allows for precise positioning of the agonist atoms as well as critical associated water molecules W2 and W3. In fact, quisqualate is bound in an identical manner in all five crystallographically independent S1S2J molecules. Close examination of the binding pocket shows that the α-carboxy and α-amino groups of all three full agonists occupy the same positions and form extensive interactions with R485, T480, and P478 in domain 1 and S654 and E705 in domain 2 (Figure 4).

However, the γ-substituents are involved in a strikingly different series of interactions. Most importantly, quisqualate faithfully mimics a glutamate-like binding mode as shown in Figure 4A, even though the shape of quisqualate's oxadiazolidine ring is more similar to the shape of AMPA's isoxazole moiety. In contrast, the quisqualate oxadiazolidine ring clearly binds in a manner different from that of the isoxazole ring of AMPA, as illustrated in Figure 4B. In particular, and as summarized in Table 3, the 3,5-dioxo-1,2,4-oxadiazolidine ring of quisqualate makes seven hydrogen bonds in the agonist-binding pocket (see Figure 1B for the numbering of the ring). The carbonyl oxygen at position 3 makes hydrogen bonds with backbone nitrogen atoms of Ser654 and Thr655 as well as with a conserved water molecule (W1), situated at the base of helix F. At the 4 position, the ring nitrogen accepts hydrogen bonds with the hydroxyl of Thr655 and a key water molecule, W2. Making the last set of hydrogen bonds to the oxadiazolidine ring is the main chain NH group of Glu705, which donates a hydrogen bond to an exocyclic oxygen bound to C5 and water W3. Interestingly, the ring oxygen, atom 1, is not involved in any <3.3 Å interactions in the binding pocket.

Table 3: Hydrogen Bond Interactions Involving Binding Sites D−F[a]

complex	**d**−S654 NH	**d**−T655 NH	**d**−W1 O	**e**−T655 OH	**e**−W2 O	**f**−E705 NH	**f**−W3 O
Quis	3.21	3.04	2.72	2.79	3.03	2.91	3.05
Glu	3.34	3.18	2.89	2.70	2.98	2.89	2.97
AMPA	3.10	3.01	2.83	2.77	3.01	3.02	3.00

[a] The hydrogen bond donors and acceptors are separated by a long dash. The letters **d**−**f** stand for the agonist atoms that are located at binding sites D−F, respectively. The distances are average values based on five quisqualate structures (this work), three glutamate structures, and three AMPA structures (*7*). The units are angstroms. The three atoms that are located at sites **d**−**f** are the oxygen atom in the 3-carbonyl group, the 4-N atom, and the oxygen atom in the 5-carbonyl group in the Quis structure; two oxygen atoms in the γ-carboxyl group and W4 in the Glu structure; and W5, the oxygen atom in the 3-carbonyl group, and the 2-N atom in the AMPA structure, respectively.

Thus, the γ-substituent of quisqualate, like the equivalent moieties of glutamate and AMPA, makes both direct and water-mediated interactions with the receptor.

Solvent Organization. The crucial solvent molecules located within 5 Å of the agonist are all present and positioned similarly in the quisqualate, glutamate, and AMPA structures, with the important exception of W4 and W5. Upon comparison of the quisqualate and glutamate structures, the oxadiazolidine ring displaces water molecule W4 from the glutamate complex; in the glutamate structure, W4 interacts with the OE2 of the γ-carboxylate, the NH group of Glu705, and W3. The oxadiazolidine ring displaces this water, and following superposition of α-carbon atoms of both structures, the oxygen attached to C5 is positioned within ∼0.55 Å of the position of W4 from the glutamate complex. There is also an important difference between the solvent organization in the quisqualate and AMPA structures, which is similar to the previously described difference in solvent organization in the glutamate and AMPA structures (*7*). In comparing the quisqualate and AMPA structures, we see that because the isoxazole ring of AMPA is positioned differently in the binding pocket, displacing W4 of the glutamate complex, AMPA binds by recruiting W5 to occupy the position of the 3-oxo group of quisqualate and the OE1 atom of glutamate. W5 therefore makes the critical bridging interactions between the backbone NH groups of Ser654 and Thr655 and the 3-hydroxyl group of AMPA.

Methionine 708. An important residue in the GluR2 binding pocket is Met708, a residue which probably plays a significant role in defining the agonist selectivity of AMPA versus kainate receptors. In the AMPA structure of GluR2 S1S2J, the 5-methyl group substantially displaces the methionine side chain away from the binding pocket, and because it is in contact with Tyr405, the side chain of Tyr405 is also displaced by ∼1.2 Å (*7*). In the quisqualate structures reported here, however, the side chain of Met708 is oriented essentially like that seen in the complexes with glutamate, with the only difference being a change in the rotomer conformation of the side chain, which is most likely due to the presence of the oxadiazolidine ring.

Peptide Bond Flip. A striking local conformational change in the agonist binding pocket that is correlated with the degree of domain closure involves the reorientation of the trans peptide bond between residues Asp651 and Ser652 (*7*). In four of the five GluR2 S1S2J−quisqualate complexes reported here, the peptide bond has "flipped" to the conformation adopted in all of the AMPA complex structures (*7*), i.e., where the N−H bond of Asp651 is oriented away from the binding pocket and the C═O bond of Ser652 is pointed toward the binding pocket. Nevertheless, molecule A of the zinc form, quisqualate complex, like molecule A of the glutamate, zinc form (*7*), does not contain a "flipped" peptide bond, perhaps because molecule A has ca. 1° less domain closure than molecules B and C due to lattice effects. In both flipped and "unflipped" states, the peptide bond between Asp651 and Ser652 is in a trans conformation, as previously described (*7*).

Subsite Map of the Binding Pocket. To simplify the discussion of the modes of agonist binding, we have created a subsite map of the agonist binding pocket, shown in Figure 5. Here we see that the γ-substituents of quisqualate, glutamate, and AMPA occupy sites D−G. Glutamate, with the smallest γ-substituent, occupies only sites D and E; a water molecule (W4) fills site F, and site G appears to be "empty", or occupied by disordered solvent. Quisqualate adopts a glutamate-like binding mode, occupying sites D−F, having displaced W4 from site F. AMPA, in contrast, occupies sites E−G, recruiting a water (W5) to site D and filling the hydrophobic site G with its 5-methyl group, in part by displacing the side chain of Met708.

DISCUSSION

Quisqualate, first identified as an excitatory amino acid nearly 30 years ago, is a potent agonist at AMPA and kainate receptors. Even though quisqualate has been employed in scores of functional studies, and was the namesake for AMPA receptors, there has been no information, at the level of three-dimensional molecular detail, about how quisqualate binds to an iGluR. In addition, there has also not been a direct comparison of the extent to which quisqualate and glutamate produce similar levels of receptor activation under conditions where desensitization is blocked. Here, we have carried out functional studies using the nondesensitizing variant (L483Y) of GluR2 in the presence of saturating quisqualate and glutamate and have measured the rates of deactivation in the context of the wild-type receptor; we have determined the IC_{50} values of quisqualate and glutamate binding using the S1S2J ligand-binding core, and we have determined the structure of the S1S2J−quisqualate complex in two different crystal forms. On the basis of these studies, we have gained new insight into the molecular determinants of agonist efficacy, potency, and specificity.

Efficacy. To compare the extent to which quisqualate and glutamate produce similar levels of receptor activation, we employed the nondesensitizing variant of the GluR2 receptor, L483Y (*44*). This mutant blocks desensitization in GluR2 as originally reported for the GluR3 receptor, thus obviating the concern that even under "rapid-solution exchange" conditions a substantial fraction of the wild-type receptor population has entered a desensitized state, for example. As illustrated in Figure 2, we see that glutamate and quisqualate

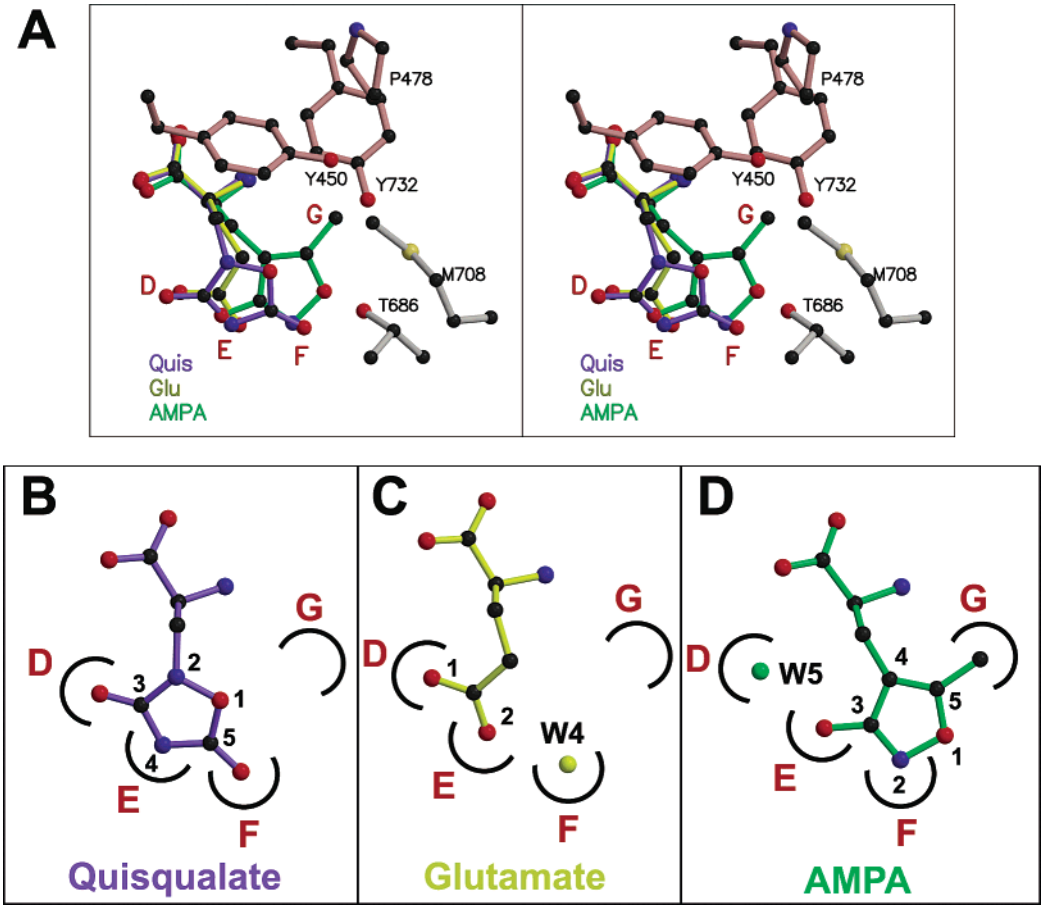

FIGURE 5: Full agonists adopt different binding modes, and water molecules play key roles in mediating agonist−receptor interactions. (A) Shown are the quisqualate (Quis, purple), glutamate (Glu, yellow), and AMPA (green) molecular structures, and the structure of the protein from the quisqualate−GluR2 S1S2J complex (domain 1 atoms in pink and domain 2 atoms in gray), following superposition of all three protein structures using α-carbon atoms in domain 1. (B) Subsite binding regions occupied by the oxadiazolidine ring of quisqualate. (C) Subsite binding regions occupied by the γ-carboxylate of glutamate and water W4. (D) Subsite binding regions occupied by the isoxasole ring of AMPA and water W5. Water molecules are shown as spheres. In panels B−D, the subsites include the following residues and atoms: Ser654 NH and Thr655 NH of subsite D, Thr655 OH of subsite E, E705 NH of subsite F, side chains of E402, Y450, P478, E705, M708, and Y732 of subsite G.

produce a similar, maximal level of receptor activation, and thus, they both behave as full agonists. In comparing the extent of domain closure produced by quisqualate, glutamate, and AMPA, we find that they all result in ca. 20° of domain closure, relative to the apo state (*7*), which is substantially more than that produced by kainate (12°), a partial agonist at AMPA receptors (*45*, *46*). Therefore, we suggest that the physiological and crystallographic data on quisqualate support our contention that the extent of domain closure is directly correlated to the extent of receptor activation and that full agonists induce the same, maximum degree of domain closure (*7*).

Potency. Even though quisqualate is similar to glutamate in terms of the level of receptor activation, i.e., quisqualate and glutamate are equally efficacious, quisqualate is a substantially more potent agonist. Indeed, while the IC_{50} of quisqualate on GluR2 S1S2J is 20 nM, the IC_{50} value for glutamate on a similar S1S2 construct is 166 nM (*16*), the K_d value for glutamate binding to S1S2J on the basis of a fluorescence assay is 180 nM (Y. Sun and E. Gouaux, unpublished results), and the IC_{50} of glutamate at an *E. coli*-expressed GluRB (GluR2) S1S2 construct is 370 nM (*42*). Furthermore, on the basis of two-electrode voltage clamp experiments using the full-length GluR2 L483Y receptor, we have shown that the EC_{50} for quisqualate is 1.2 μM and the EC_{50} for glutamate is 20 μM. Rapid perfusion experiments with membrane patches from HEK cells transfected with GluR2 reveal that, following the removal of agonist, GluR2 channels close 6 times faster for glutamate than for quisqualate, consistent with an increase in the stability of the GluR2−quisqualate complex. Thus, we sought to understand why quisqualate binds to and activates GluR2 at concentrations ∼10-fold lower than those required for equivalent glutamate binding and activation.

On the basis of the data presented in Table 3 and Figure 5, we see that quisqualate makes the same interactions with the receptor binding subsites as does glutamate and water molecule W4. In fact, the distances between the receptor and the analogous atoms in the quisqualate and glutamate complexes are very similar, and thus, one might consider glutamate with W4 as an isosteric analogue of quisqualate. A plausible explanation for why quisqualate binds more tightly to the receptor than glutamate is that the displacement of water W4 by the oxadiazolidine ring is entropically favorable; the tightly bound water is released into solution and gains translational and rotational degrees of freedom (*47*). In addition, because quisqualate incorporates the equivalent of W4 into a rigid, preorganized ring, dissociation of the γ-substituent requires breaking of four protein−ligand hydrogen bonds, while for the glutamate complex, dissocia-

tion of the γ-COOH group breaks three protein−ligand hydrogen bonds and a ligand−solvent−protein hydrogen bond.

AMPA also recruits a water molecule in its binding to GluR2 S1S2. However, in this instance, the water occupies site D, while the isoxazole atoms are positioned in sites E−G. AMPA, which also binds to the receptor ca. 10-fold more tightly than glutamate, probably does so, at least in part, due to the burial of the hydrophobic methyl group in pocket G. On the basis of the quisqualate, glutamate, and AMPA structures, one would predict that an agonist that occupied all four sites, without the requirement for the recruitment of a water molecule, would bind to the receptor even more strongly than quisqualate and AMPA and, if it produced maximal domain closure, would fully activate the ion channel.

Specificity. One of the distinguishing features of quisqualate is that it is not specific for AMPA versus kainate receptors, much like glutamate. In contrast, AMPA possesses much greater receptor subtype specificity. The reason quisqualate and glutamate behave similarly is almost certainly due to the fact that quisqualate and glutamate bind to both AMPA and kainate receptors in a similar mode; i.e., we predict that the γ-substituents of quisqualate and glutamate will occupy the equivalent of sites D−F in kainate receptors. In kainate receptors, we suggest that there will also be an equivalent to water W4 of the GluR2 S1S2J−glutamate complex that is displaced upon quisqualate binding. Of course, an important constraint on the binding of agonists to subsites D−F comes from the fact that these sites, to a large extent, are defined by main chain atoms that are predominately NH groups.

AMPA, as well as other agonists that might exploit subsite G, such as the willardiines (*48*, *49*), shows greater receptor subtype specificity because the atoms that compose subsite G are primarily side chain atoms, and the corresponding residues vary between AMPA and kainate receptors. For example, in the rat AMPA receptors, residue 708 is a methionine, which complements the 5-methyl group of AMPA. However, kainate receptors typically have a smaller, polar residue at this position, a serine in GluR5 and a threonine in GluR6 and GluR7 (*50*−*52*). Therefore, kainate receptors have a larger, more polar subsite G. In addition to the composition of subsite G, kainate receptors also exhibit differences in residues that occupy sites that, in GluR2 S1S2J, are close to the γ-substituent binding site. One such residue, Thr686, is a serine in GluR5 and an asparagine in GluR6. Substitution of the asparagine at this site with serine, in GluR6, confers sensitivity to AMPA (*53*) and (*S*)-5-iodowillardiine (*54*). Residues at sites that are equivalent to position 686 in the GluR2 receptor probably alter receptor specificity because they are in positions not only to interact with crucial water molecules in the agonist binding pocket but also to mediate important domain 1−domain 2 interactions. These interdomain contacts, in turn, are required for stabilizing the closed-cleft, activated form of the receptor (*20*).

In conclusion, the crystal structure of the GluR2 ligand-binding core in complex with quisqualate has been determined at high resolution, and complementary binding and physiology experiments have been carried out. Quisqualate induces a fully closed domain conformation which is similar to the AMPA and glutamate structures. This observation supports our theory that full agonists induce similar conformational changes in the ligand-binding core. Structure comparisons among full agonist structures reveal that water molecules play important roles in mediating agonist−receptor interactions and that a partially hydrophobic pocket near the γ-substituents of agonists is important for determination of receptor subtype specificity. The relative affinity of glutamate for the receptor appears to be well suited to high-frequency synaptic signaling, to a large degree because glutamate enables rapid deactivation of the receptor, thus minimizing the accumulation of densensitized forms of the receptor. Quisqualate, in contrast, results in slowly deactivating, strongly desensitizing responses, and therefore, high-frequency stimulation of the receptor by agonists such as quisqualate would result in the buildup of receptor populations in inactive, desensitized states.

ACKNOWLEDGMENT

Neali Armstrong is gratefully acknowledged for measuring the quisqualate dose−response data. Joe Lidestri is acknowledged for support of the X-ray facilities at Columbia University. Craig Ogata and Randy Abramowitz are thanked for assistance with X-ray data collection at X4A, which is located at the National Synchrotron Light Source, Brookhaven National Laboratory (Upton, NY). Carla Glasser provided technical support for the physiology experiments.

SUPPORTING INFORMATION AVAILABLE

Index of key residues and water molecules in the PDB files. This material is available free of charge via the Internet at http://pubs.acs.org.

REFERENCES

1. Chen, G.-Q., Cui, C., Mayer, M., and Gouaux, E. (1999) *Nature 402*, 817−821.
2. Mayer, M. L., Olson, R. A., and Gouaux, E. (2001) *J. Mol. Biol. 311*, 815−836.
3. Dingledine, R., Borges, K., Bowie, D., and Traynelis, S. F. (1999) *Pharmacol. Rev. 51*, 7−61.
4. Hollmann, M., and Heinemann, S. (1994) *Annu. Rev. Neurosci. 17*, 31−108.
5. Seeburg, P. H. (1993) *Trends Neurosci. 16*, 359−365.
6. Rosenmund, C., Stern-Bach, Y., and Stevens, C. F. (1998) *Science 280*, 1596−1599.
7. Armstrong, N., and Gouaux, E. (2000) *Neuron 28*, 165−181.
8. Robert, A., Irizarry, S. N., Hughes, T. E., and Howe, J. R. (2001) *J. Neurosci. 21*, 5574−5586.
9. Ayalon, G., and Stern-Bach, Y. (2001) *Neuron 31*, 103−113.
10. Madden, D. R. (2002) *Nat. Rev. Neurosci. 3*, 91−101.
11. Hollmann, M., Maron, C., and Heinemann, S. (1994) *Neuron 13*, 1331−1343.
12. Stern-Bach, Y., Bettler, B., Hartley, M., Sheppard, P. O., O'Hara, P. J., and Heinemann, S. F. (1994) *Neuron 13*, 1345−1357.
13. Kuusinen, A., Arvola, M., and Keinänen, K. (1995) *EMBO J. 14*, 6327−6332.
14. Wo, Z. G., and Oswald, R. E. (1995) *Trends Neurosci. 18*, 161−168.
15. Paas, Y. (1998) *Trends Neurosci. 21*, 117−125.
16. Chen, G. Q., and Gouaux, E. (1997) *Proc. Natl. Acad. Sci. U.S.A. 94*, 13431−13436.
17. Chen, G.-Q., Sun, Y., Jin, R., and Gouaux, E. (1998) *Protein Sci. 7*, 2623−2630.
18. Armstrong, N., Sun, Y., Chen, G.-Q., and Gouaux, E. (1998) *Nature 395*, 913−917.
19. McFeeters, R. L., and Oswald, R. E. (2002) *Biochemistry 41*, 10472−10481.
20. Sun, Y., Olson, R. A., Horning, M., Armstrong, N., Mayer, M. L., and Gouaux, E. (2002) *Nature 417*, 245−253.

21. Takemoto, T. (1978) in *Kainic Acid as a Tool in Neurobiology* (McGeer, E. G., Olney, J. W., and McGeer, P. L., Eds.) pp 1−15, Raven, New York.
22. Johnston, G. A. R., Curtis, D. R., Davies, J., and McCulloch, R. M. (1974) *Nature 248*, 804−805.
23. Davies, J., and Watkins, J. C. (1981) *Brain Res. 206*, 172−177.
24. Monaghan, D. T., Bridges, R. J., and Cotman, C. W. (1989) *Annu. Rev. Pharmacol. Toxicol. 29*, 365−402.
25. Sugiyama, H., Ito, I., and Hirono, C. (1987) *Nature 325*, 531−533.
26. Krogsgaard-Larsen, P., Honore, T., Hansen, J. J., Curtis, D. R., and Lodge, D. (1980) *Nature 284*, 64−66.
27. Hollmann, M., O'Shea-Greenfield, A., Rogers, S. W., and Heinemann, S. (1989) *Nature 342*, 643−648.
28. Chen, G.-Q., and Gouaux, E. (2000) *Tetrahedron 56*, 9409−9419.
29. Otwinowsky, Z., and Minor, W. (1997) *Methods Enzymol. 276*, 307−326.
30. Navaza, J. (1994) *Acta Crystallogr. A50*, 157−163.
31. Brunger, A. T., Adams, P. D., Clore, G. M., DeLano, W. L., Gros, P., Grosse-Kunstleve, R. W., Jiang, J. S., Kuszewski, J., Nilges, M., Pannu, N. S., Read, R. J., Rice, L. M., Simonson, T., and Warren, G. L. (1998) *Acta Crystallogr. D54*, 905−921.
32. Jones, T. A., and Kjeldgaard, M. (1997) *Methods Enzymol. 277*, 173−208.
33. Jones, T. A., Zou, J.-Y., and Cowan, S. W. (1991) *Acta Crystallogr. A47*, 110−119.
34. Brünger, A. T. (1992) *Nature 355*, 472−475.
35. Kleywegt, G. J. (1999) *Acta Crystallogr. D55*, 1878−1884.
36. Lu, G. (2001) http://bioinfo1.mbfys.lu.se/∼guoguang/fit.html.
37. Kraulis, P. J. (1991) *J. Appl. Crystallogr. 24*, 946−950.
38. Esnouf, R. M. (1999) *Acta Crystallogr. D55*, 938−940.
39. Merritt, E. A., and Murphy, M. E. P. (1994) *Acta Crystallogr. D50*, 869−873.
40. Keinänen, K., Wisden, W., Sommer, B., Werner, P., Herb, A., Verdoorn, T. A., Sakmann, B., and Seeburg, P. H. (1990) *Science 249*, 556−560.
41. Schreibmayer, W., Lester, H. A., and Dascal, N. (1994) *Pfluegers Arch. 426*, 453−458.
42. Arvola, M., and Keinänen, K. (1996) *J. Biol. Chem. 271*, 15527−15532.
43. Keinänen, K., Köhr, G., Seeburg, P. H., Laukkanen, M.-L., and Oker-Blom, C. (1994) *Bio/Technology 12*, 802−806.
44. Stern-Bach, Y., Russo, S., Neuman, M., and Rosenmund, C. (1998) *Neuron 21*, 907−918.
45. Kiskin, N. I., Krishtal, O. A., and Tsyndrenko, A. Y. (1986) *Neurosci. Lett. 63*, 225−230.
46. Patneau, D. K., and Mayer, M. L. (1991) *Neuron 6*, 785−798.
47. Fersht, A. (1999) *Structure and Mechanism in Protein Science*, W. H. Freeman and Co., New York.
48. Patneau, D. K., Mayer, M. L., Jane, D. E., and Watkins, J. C. (1992) *J. Neurosci. 12*, 595−606.
49. Wong, L. A., Mayer, M. L., Jane, D. E., and Watkins, J. C. (1994) *J. Neurosci. 14*, 3881−3897.
50. Bettler, B., Egebjerg, J., Sharma, G., Pecht, G., Hermans-Borgmeyer, I., Moll, C., Stevens, C. F., and Heinemann, S. (1992) *Neuron 8*, 257−265.
51. Egebjerg, J., Bettler, B., Hermans-Borgmeyer, I., and Heinemann, S. (1991) *Nature 351*, 745−748.
52. Bettler, B., Boulter, J., Hermans-Borgmeyer, I., O'Shea-Greenfield, A., Deneris, E. S., Moll, C., Borgmeyer, U., Hollmann, M., and Heinemann, S. (1990) *Neuron 5*, 583−595.
53. Swanson, G. T., Gereau, R. W., Green, T., and Heinemann, S. F. (1997) *Neuron 19*, 913−926.
54. Swanson, G. T., Green, T., and Heinemann, S. F. (1998) *Mol. Pharmacol. 53*, 942−949.

BI020583K